MPMI Vol. 28, No. 5, 2015, pp. 534–545. http://dx.doi.org/10.1094/MPMI-11-14-0354-R

e-Xtra*

A *Lotus japonicus* Cochaperone Protein Interacts With the Ubiquitin-Like Domain Protein CIP73 and Plays a Negative Regulatory Role in Nodulation

Heng Kang,[1,2] Aifang Xiao,[2] Xiaoqin Huang,[2] Xioumei Gao,[2] Haixiang Yu,[2] Xingxing He,[2] Hui Zhu,[2] Zonglie Hong,[3] and Zhongming Zhang[2]

[1]Institute of Applied Mycology, College of Plant Science and Technology, Huazhong Agricultural University, Wuhan 430070, China; [2]State Key Laboratory of Agricultural Microbiology, Huazhong Agricultural University, Wuhan 430070, China; [3]Department of Plant, Soil, and Entomological Sciences and Program of Microbiology, Molecular Biology and Biochemistry, University of Idaho, Moscow, ID 83844-2339, U.S.A.

Submitted 3 November 2014. Accepted 21 December 2014.

The calcium/calmodulin-dependent protein kinase CCaMK forms a complex with its phosphorylation target CIP73 (CCaMK-interacting protein of 73 kDa). In this work, a homolog of the animal HSC/HSP70 interacting protein (HIP) was identified as an interacting partner of CIP73 in *Lotus japonicus*. *L. japonicus* HIP contains all functional domains characteristic of animal HIP proteins. The C-terminal STI1-like domain of *L. japonicus* HIP was found to be necessary and sufficient for interaction with CIP73. The interaction between CIP73 and HIP occurred in both the nuclei and cytoplasm in *Nicotiana benthamiana* leaf cells. The interactions between CIP73 and HIP and between CIP73 and CCaMK could take place simultaneously in the same nuclei. *HIP* transcripts were detected in all plant tissues tested. As nodule primordia developed into young nodules, the expression of *HIP* was downregulated and the *HIP* transcript level became very low in mature nodules. More nodules were formed in transgenic hairy roots of *L. japonicus* expressing *HIP* RNA interference at 16 days postinoculation as compared with the control hairy roots expressing the empty vector. It appears that HIP may play a role as a negative regulator for nodulation.

Legume plants have evolved with two types of mutualistic plant-microbe interactions, arbuscular mycorrhizal symbiosis (AMS) with fungi and root nodule symbiosis (RNS) with soil rhizobia. RNS and AMS supply the host plants with nitrogen and phosphate nutrients, both having agronomic and ecologic importance. Despite of the difference in fungal and bacterial symbionts, genetic dissections of AMS and RNS using model legumes, including *Lotus japonicus* and *Medicago truncatula*, have revealed that both types of symbioses share overlap components of the signaling pathway, composing the "common symbiosis pathway (CSP)" (Oldroyd 2013). Calcium and calmodulin (CaM)-dependent protein kinases (CCaMK) play a crucial role among the CSP (Lévy et al. 2004).

Ca^{2+}-spiking is one of the earliest cellular responses in both AMS and RNS and consists of periodic increases of calcium concentration in the perinuclear and nuclear regions (Capoen et al. 2011; Harper and Harmon 2005; Miwa et al. 2006). CCaMK acts as the decoder of Ca^{2+}-spiking and has the peptide structure features that are consistent with its biochemical function, including a serine/threonine kinase domain, a CaM-binding domain, and three visinin-like EF-hand motifs that trap Ca^{2+} ions (Ramachandiran et al. 1997; Takezawa et al. 1996). The N-terminal part of plant CCaMK resembles the animal CaM II, which is able to decode Ca^{2+}-spiking involved in the neuronal signaling pathway (De Koninck and Schulman 1998). CCaMK are highly conserved in plants, including *M. truncatula*, *L. japonicus*, and *Sesbania rostrata* (Capoen et al. 2009; Godfroy et al. 2006; Lévy et al. 2004; Poovaiah et al. 1999; Tirichine et al. 2006). Rice CCaMK is required for AMS and can also functionally complement legume CCaMK knock-out mutations, indicating an equivalent role of CCaMK homologs in nonlegumes (Chen et al. 2007; Godfroy et al. 2006).

Recent biochemical and genetic studies of plant CCaMK have provided new insight into the molecular mechanism for decoding Ca^{2+}-spiking (Miller et al. 2013). In the absence of Ca^{2+}, CCaMK remains in an autoinhibited state. Binding of Ca^{2+} to the EF-hand motifs induces autophosphorylation at a conserved threonine residue in the kinase domain (T265 in *L. japonicus* CCaMK) to release autoinhibition, which enables high-affinity CaM binding and, consequently, substrate phosphorylation (Ramachandiran et al. 1997; Sathyanarayanan et al. 2001). Deregulation of CCaMK by the point mutation in the autophosphorylation site of the kinase domain or deletion of the C-terminal CaM-binding and EF-hands motifs leads to the development of spontaneous nodules in the absence of rhizobia (Gleason et al. 2006; Tirichine et al. 2006). Further detailed genetic analyses have revealed that the deregulated version of $CCaMK^{T265D}$ or *snf1* ($CCaMK^{T265I}$) can rescue Ca^{2+}-spiking-deficient mutants, including *symrk*, *castor*, *pollux*, *nup85*, and *nup133* in RNS and AMS (Hayashi et al. 2010; Madsen et al. 2010). On the other hand, expression of the sole kinase domain fused to a nuclear localization signal, lacking the autoinhibitory domain, has been shown to be sufficient for spontaneous nodulation and AM development but not for rhizobial infection (Shimoda et al. 2012; Takeda et al. 2012). Recently, a new autophosphorylation site has

Heng Kang and Aifang Xiao contributed equally to this work.

The sequence data for *HIP* is available in GenBank under accession number KF723716.

Corresponding author: Zhongming Zhang; E-mail: zmzhang@mail.hzau.edu.cn; Telephone: +86.027.8728.1687; Fax: +86.027.8728.0670.

*The *e*-Xtra logo stands for "electronic extra" and indicates that seven supplementary figures and one supplementary table are published online.

been identified in the CaM-binding domain of CcaMK, both in *L. japonicus* and *M. truncatula* (Liao et al. 2012; Routray et al. 2013). Phosphorylation of this site negatively affects the interaction of CCaMK with CaM and IPD3 and blocks RNS, AMS, and spontaneous nodulation activity of $CCaMK^{T271A}$ in *M. truncatula* (Routray et al. 2013).

Work aimed at screening targets of CCaMK has led to identification of CYCLOPS/IPD3 and CIP73, both serving as phosphorylation substrates of CCaMK (Kang et al. 2011; Messinese et al. 2007; Yano et al. 2008). CYCLOPS/IPD3 is a coiled-coil nuclear protein, while CIP73 is a Scythe-N domain-containing, ubiquitin-like protein with unknown functions. The *cyclops* mutants can form nodule primordia but are impaired in rhizobial infection and mycorrhization (Yano et al. 2008). The *ipd3* mutants of two *Medicago* ecotypes, Jemalong and R108, are somewhat different in phenotype. Although both ecotypes can develop uninfected nodules, Jemalong but not R108 forms infection threads but fails to develop symbiosomes and does not express symbiosomal membrance marker SYMREM1 (Horváth et al. 2011; Lefebvre et al. 2010; Ovchinnikova et al. 2011). RNA interference (RNAi)-mediated knockdown of CIP73 expression leads to impaired RNS (Kang et al. 2011). However, how CYCLOPS and CIP73 regulate the function of CCaMK at the biochemical and molecular levels remains unknown.

Animal HSC/HSP70-interacting protein (HIP) interacts with the ATPase domain of heat shock cognate 70 (HSC70) and is part of the progesterone receptor-chaperone complexes (Höhfeld et al. 1995; Prapapanich et al. 1996b; Smith 1993). In this work, we report the identification of a homolog of eukaryotic HIP as an interacting partner of CIP73 in *L. japonicus*. *L. japonicus* HIP was colocalized with CCaMK and CIP73 in the nuclei. RNAi-mediated knockdown of *HIP* expression in *L. japonicus* hairy roots led to increased nodule formation. These results demonstrate a role of *L. japonicus* HIP as a negative regulator of nodulation in legume plants.

RESULTS

Identification of HIP as an interacting partner of CIP73.

CIP73 has previously been identified as a CCaMK-interacting protein (Kang et al. 2011). In this work, we used the yeast two-hybrid system to identify potential interacting partners of CIP73. When fused to the Gal4 DNA binding domain, the full-length CIP73 caused autoactivation of the Gal4 system and could not be used to screen the library. The C-terminus of CIP73 (414 to 691) did not cause this autoactivation and was used as bait to screen a *L. japonicus* root cDNA library (Zhu et al. 2008). Under stringent screen conditions, a total of 16 independent clones were isolated, and they contained different lengths of inserts, all derived from the same gene (Supplementary Fig. 1). One of them contained a full-length coding sequence encoding a peptide that shares 47% amino acid identity with the human HIP (Höhfeld et al. 1995). The gene was thus designated as *L. japonicus HIP*, the cDNA sequence of which was deposited to GenBank under accession number KF723716.

Structure features of HIP protein.

The deduced peptide sequence of *L. japonicus* HIP consists of 418 amino acids, with a calculated molecular mass of 44.7 kDa. It contains all functional domains of animal HIP proteins, including a conserved N-terminal dimerization domain, a highly acidic domain, three tetratricopeptide repeats (TPR), a charged region, a series of degenerate glycine-glycine-methionine-proline (GGMP) tandem repeats, and a C-terminal region with limited similarity to yeast stress–induced protein Sti1 and its ortholog HOP/p60 (Fig. 1A). The TPR domain of animal HIP proteins may mediate interactions with heat shock proteins (Carrello et al. 2004; Hernández Torres et al. 2009; Velten et al. 2000), while the exact function of the GGMP repeats is unclear (Boorstein et al. 1994). HIP homologs are present in protists, plants, and animals (Supplementary Table 1) but absent in fungi and algae. Some plant species, such as soybean, poplar, and tobacco, contain a pair of HIP proteins, designated as HIPa and HIPb, that appear to arise from apparent genome duplication. Analysis of HIP protein alignment reveals a high degree of sequence conservation from animals to plants (Supplementary Fig. 2). The phylogenetic tree of HIP proteins divides into different clusters that perfectly fit within their kingdoms, indicating the evolutionary conservation of *HIP* genes (Fig. 1B). Interestingly, HIP proteins in brassicas and legumes present notable divergence from other dicot species (Fig. 1B).

The Sti1-like domain of HIP is sufficient for interaction with CIP73.

From the library screen, the HIP clone with the shortest coding region (355 to 418 aa) contained only the C-terminal Sti1-like domain, indicating that this C-terminal domain is sufficient for interaction with CIP73. We made different deletions of both CIP73 and HIP in order to dissect domains required for the interaction (Fig. 2A). We detected that the C-terminus of CIP73 (CIP73-C) interacted with both the full-length HIP and the C-terminal Sti1-like domain (HIP-C) but not with the N-terminus of HIP (HIP-N) (Fig. 2B), indicating that the C-terminal Sti1-like domain of HIP is necessary and sufficient for interaction with CIP73. Because the full-length CIP73 fused with the Gal4 DNA-binding domain led to autoactivation in the yeast system, we switched the Gal4 activation domain to the full-length CIP73 and the binding domain to HIP. The result showed that yeast colonies harboring this combination were able to grow on the selection medium lacking His and Ade (SD/-Trp-Leu-His-Ade) and exhibited significant β-galactosidase activities on medium containing X-Gal (Fig. 2B). These results suggest that both CIP73-C and full-length CIP73 are able to interact with HIP.

The interaction between CIP73 and HIP was further confirmed by an in vitro protein pull-down assay. The full-length HIP and its deletion fragments HIP-N and HIP-C were expressed as chitin-binding domain (CBD) fusion proteins. CIP73 was expressed as 6×His tagged recombinant protein in *Escherichia coli* cells. HIP and its deletion fragments were absorbed on chitin beads and were used to incubate with purified soluble CIP73. After washing with buffer, proteins retained on the beads were eluted and resolved by sodium dodecyl sulfate-polyacrylamide gel electrophoresis (SDS-PAGE). The presence of CIP73 on the beads was detected by immunoblotting with anti-His tag antibody. Only the full-length HIP and its C-terminal HIP-C could pull down CIP73, confirming that the C-terminal domain of HIP is responsible for interacting with CIP73 (Fig. 2C).

Interaction between HIP and CIP73 in planta.

We used bimolecular fluorescence complementation (BiFC) assay to test whether the interaction between CIP73 and HIP took place in plant cells. Proteins fused to the C- or N-terminal yellow fluorescence protein (YFPC and YFPN, respectively) were coexpressed in *Nicotiana benthamiana* epidermal leaf cells. The expression of recombinant proteins in *N. benthamiana* leaves was confirmed by immunoblot analysis using anti-hemagglutinin (HA) and anti-c-myc monoclonal antibodies (Fig. 3G). Coexpression of YFPC-CIP73 and HIP-YFPN led to strong yellow fluorescence signals in both the cytoplasm and nucleus (Fig. 3A), suggesting a positive interaction between CIP73 and HIP in plant cells. The interaction was further confirmed when the split YFP tags were switched between CIP73 and HIP,

although the fluorescence intensity was weaker (Fig. 3B). Because the N-terminal HIP (HIPN) did not interact with CIP73 in yeast cells and in protein pull-down assays (Fig. 2B and C), the combinations of YFPC-CIP73 with HIPN-YFPN (Fig. 3C) and YFPC-HIPN with CIP73-YFPN (Fig. 3D) were used as negative controls and no significant fluorescence signals were detected.

Homodimerization of HIP.

To test if HIP formed homodimers in planta, full-length HIP or its N-terminus (HIPN) was fused with the split YFP tags and was expressed in *N. benthamiana* leaf cells. Coexpression of YFPC-HIP and HIP-YFPN (Fig. 3E) or YFPC-HIPN and HIPN-YFPN (Fig. 3F) resulted in significant fluorescence signals in both the cytoplasm and nucleus, suggesting the formation of a homodimer via the N-terminus of HIP protein. This observation is consistent with the previous report on the homodimerization of rat HIP (Irmer and Höhfeld 1997).

Subcellular localization of HIP.

From the BiFC result, HIP appeared to distribute between the cytoplasm and nucleus when coexpressed with CIP73 (Fig. 3A and B) or expressed alone (Fig. 3E and F), which is different from the cytoplasmic localization pattern of rat HIP (Höhfeld et al. 1995). We examined the subcellular localization of *L. japonicus* HIP in *N. benthamiana* leaf epidermal cells expressing HIP-GFP under the control of the *Cauliflower mosaic virus* (CaMV) 35S promoter (35S::HIP-GFP). GFP-tagged HIP was localized in both the cytoplasm and nucleus (Fig. 4B), consistent with the BiFC analysis (Fig. 3). Similar subcellular localization patterns (Fig. 4D) were also observed when HIP-GFP was expressed in *N. benthamiana* leaf cells under the control of the *L. japonicus HIP* native promoter

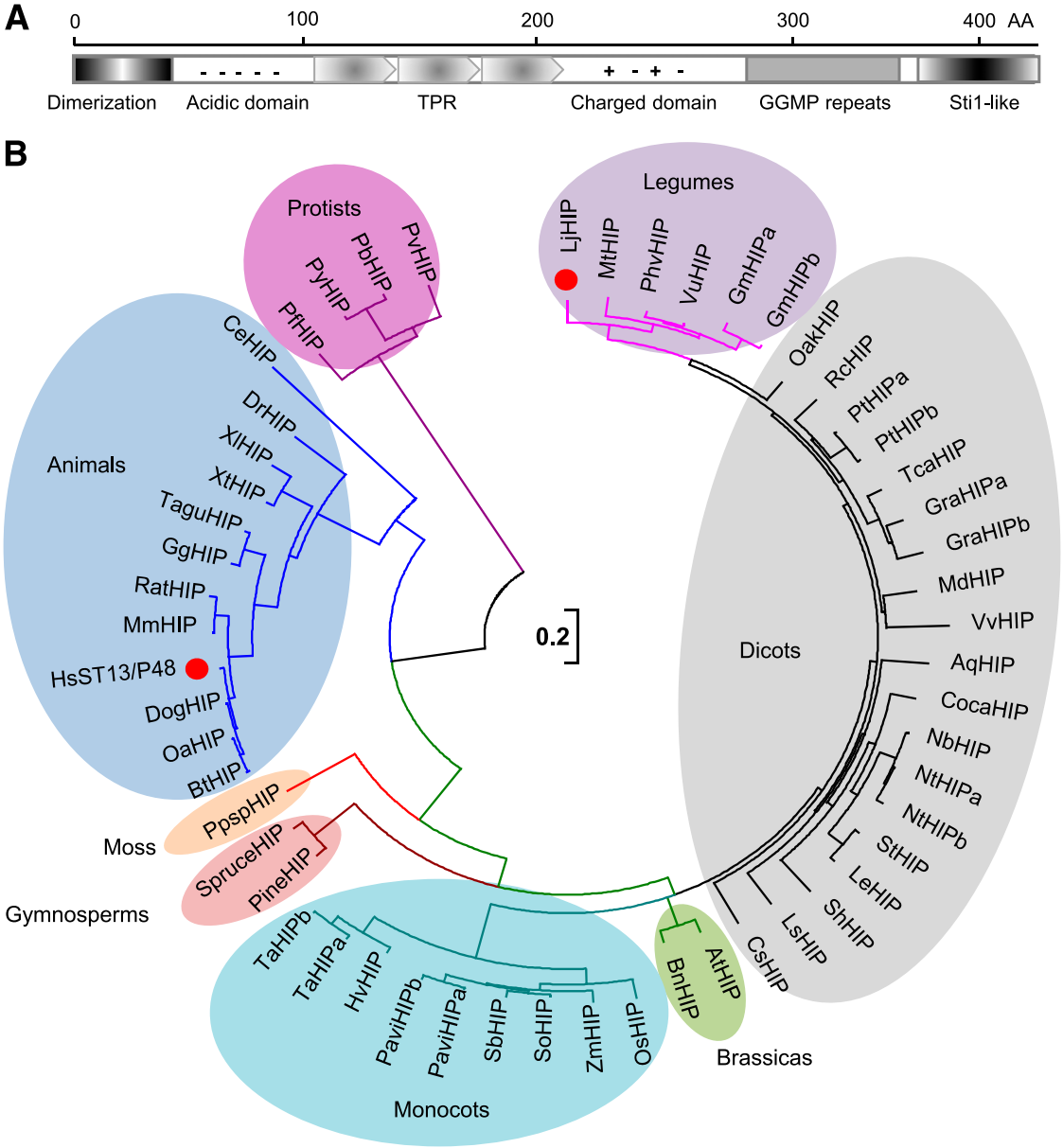

Fig. 1. HSC/HSP70 interacting protein (HIP) homologs in eukaryotes. **A,** Schematic illustrations of functional domains of HIP protein. HIP contains 418 amino acid residues with an N-terminal dimerization domain, an acidic domain, three tetratricopeptide repeats (TPR), a highly charged region, a series of degenerate glycine-glycine-methionine-proline (GGMP) repeats, and a C-terminal Sti1-like region similar to the Sti1/HOP/p60 protein. **B,** A phylogenetic tree of HIP homologous proteins from animals, plants, and protists. Note that in the plant kingdom, brassicas and legumes are divergent from other dicots. Dots highlight LjHIP, which is the subject of this work, and HsST13/P48, which has been characterized in animals with regard to its biological function and could be useful to future work to understand the function of HIP proteins in plants. The scale bar is an indicator of genetic distance based on branch length.

(*HIP*pro::HIP-GFP). Because free GFP cleaved from the fusion product might also result in the cytoplasmic and nuclear localization patterns, we examined the HIP-GFP fusion protein product using immunoblot with anti-GFP antibody. The HIP-GFP fusion protein was found to be intact (Supplementary Fig. 4).

To determine the subcellular localization of HIP in *L. japonicus* roots, we generated transgenic hairy roots expressing *HIP*pro::HIP-GFP or 35S::HIP-GFP (Fig. 4E). Similar to the observation in *N. benthamiana* leaf cells, fluorescent signals of HIP-GFP were found in both the cytoplasm and nuclei in the hairy roots of *L. japonicus* (Fig. 4E). The fluorescent signal of *HIP*pro::HIP-GFP was weaker than that of 35S::HIP-GFP (data not shown). The subcellular localization pattern of HIP-GFP was not altered three days after inoculation with *Mesorhizobium loti* (Supplementary Fig. 5).

Colocalization of CIP73 with HIP and CCaMK in the nuclei.

CIP73 and CCaMK were shown to localize in the nucleus (Kang et al. 2011; Takeda et al. 2012), while HIP was localized in both the nucleus and cytoplasm (Fig. 4). Therefore, we tested whether CIP73, HIP, and CCaMK would colocalize in *N. benthamiana* leaf cells. We first tested subcellular localization of each protein fused with GFP or mCherry under the control of the 35S promoter. The fluorescent signal of CIP73-GFP and CIP73-mCherry was found in the nucleus (Supplementary Fig. 3A and B). As a control, CYCLOPS, an interacting partner of CCaMK, exhibited similar subcellular localization to CIP73. Interestingly, CCaMK showed a low level of cytoplasmic fluorescence in addition to the strong nuclear signal. To avoid any potential undesirable effect of protein overexpression driven by the 35S promoter, we also investigated the subcellular distribution of CCaMK under the CCaMK native promoter. Similar subcellular localization patterns of CCaMK were observed when the CCaMK native promoter was used.

When coexpressed in *N. benthamiana* leaf cells, CIP73-GFP and CCaMK-mCherry showed excellent colocalization in the nuclei (Fig. 5A). CIP73-GFP and HIP-mCherry were found to colocalize in the nuclei (Fig. 5B). Both CCaMK-mCherry and HIP-mCherry exhibited a slightly diminished signal of cytoplasmic localization

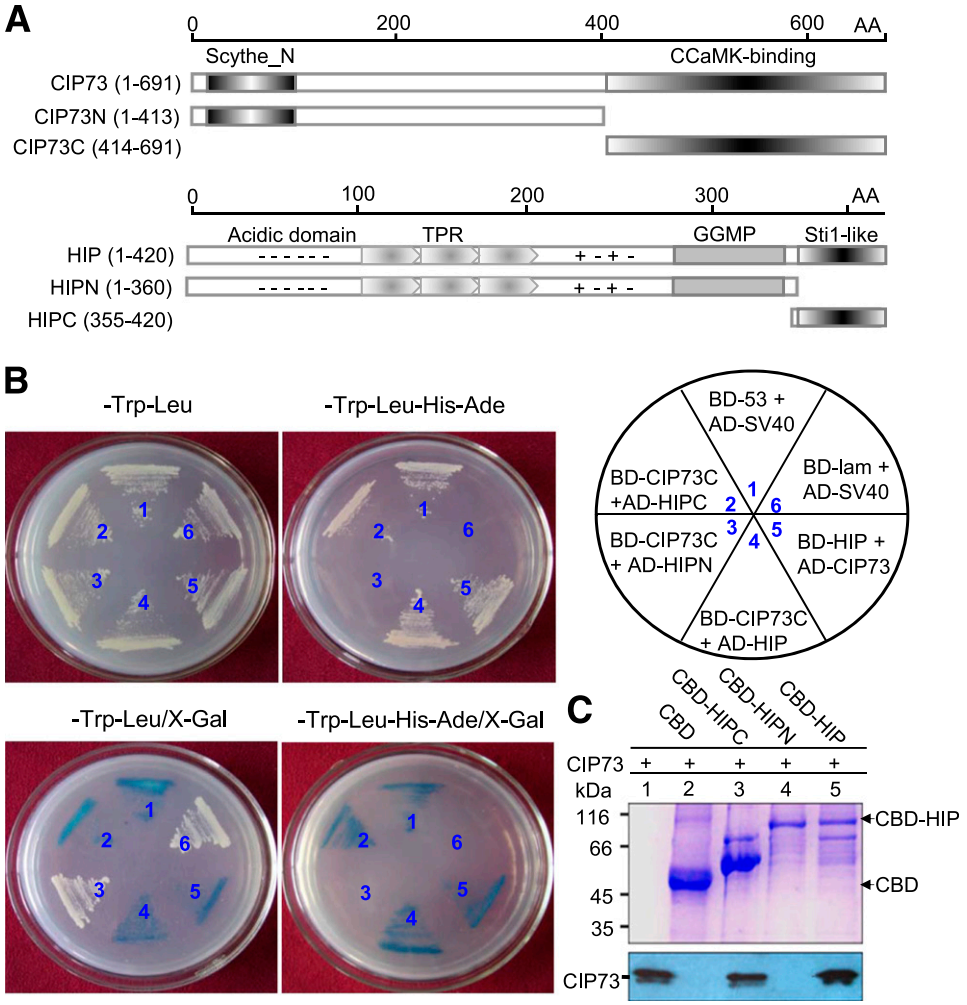

Fig. 2. Interaction of HSC/HSP70 interacting protein (HIP) with CIP73. **A,** Schematic illustrations of CIP73 and HIP deletion constructs. The C-terminal calcium and calmodulin-dependent protein kinase (CCaMK)-binding domain of CIP73 (aa 414 to 691) was used as bait for isolation of HIP from the two-hybrid library. **B,** Dissection of functional domains of HIP required for interacting with CIP73. Yeast colonies containing the bait and prey constructs were selected on SD/-Trp-Leu medium, while colonies with positive protein-protein interactions were tested on SD/-Trp-Leu-His-Ade medium. The interaction strength was measured through the β-galactosidase activity on plates containing X-Gal (80 μg ml^{-1}). The combination of BD-53/AD-SV40 was used as a positive control and BD-Lam/AD-SV40 as a negative control (Clontech). Note that the Sti1-like domain (HIPC) of HIP was necessary and sufficient for interaction with CIP73. BD, Gal4 DNA binding domain; AD, Gal4 activation domain. **C,** Protein pull-down assay for the interaction between CIP73 and HIP. His-tagged CIP73 was incubated with the immobilized chitin-binding domain (CBD)-HIP, CBD-HIP truncated proteins, or CBD alone. After washing, the proteins were separated on sodium dodecyl sulfate-polyacrylamide gel electrophoresis and were visualized by staining with Coomassie brilliant blue R250 (top). A similar gel was used for immunoblot with anti-His-tag antibody (bottom). Lane 1 is a positive control that contained a diluted sample of purified His-CIP73 protein. The positions of CBD and CBD-tagged HIP proteins on the Coomassie-stained gels are indicated by arrows.

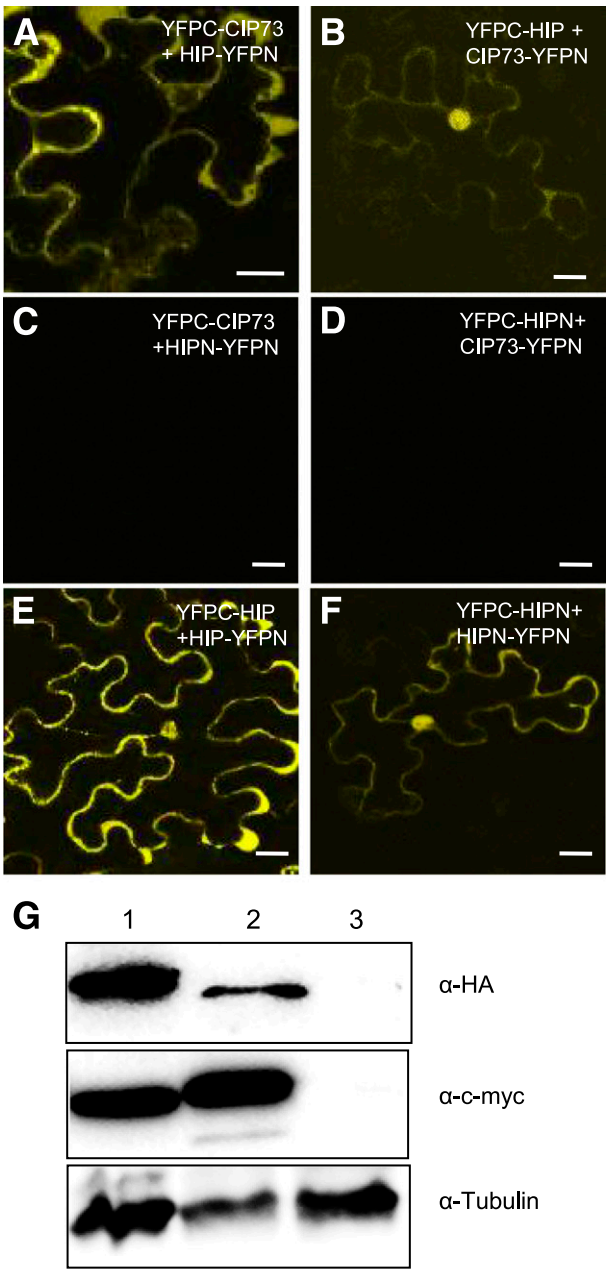

Fig. 3. Interaction between CIP73 and HSC/HSP70 interacting protein (HIP) and homodimerization of HIP in planta. **A** to **D,** Interaction between CIP73 and HIP in planta. CIP73 and HIP were expressed in *Nicotiana benthamiana* leaves as fusion proteins with the C-terminal yellow fluorescent protein (YFP) and N-terminal YFP, respectively. Coexpression of YFPC-CIP73 and HIP-YFPN led to strong fluorescence signals in both the cytoplasm and nucleus (A). The interaction was further confirmed by switching the split YFP tags between CIP73 and HIP (B). Coexpression of YFPC-CIP73 and HIPN-YFPN (C) and coexpression of YFPC-HIPN and CIP73-YFPN (D) served as negative controls. **E** to **F,** Homodimerization of HIP in planta. Full-length HIP or its N-terminal dimerization domain (HIPN) was fused with the split YFP tags. Coexpression of YFPC-HIP and HIP-YFPN (E) and YFPC-HIPN with HIPN-YFPN (F) resulted in strong fluorescence signals in both the cytoplasm and nucleus. Images were taken 3 days postinfiltration with *Agrobacterium* cells harboring appropriate expression plasmids. **G,** Immunoblot analysis of proteins expressed in *N. benthamiana* leaves. Anti-hemagglutinin (HA) and anti-c-myc antibodies detected the HA and c-myc tags present in the YFPC and YFPN domains, respectively. Antitubulin antibody was used for protein loading references. Lane 1, leaf extract expressing YFPC-CIP73 and HIPN-YFPN; Lane 2, leaf extract expressing YFPC-CIP73 and HIP-YFPN; Lane 3, control leaf. Scale bars represent 20 μm.

when coexpressed with CIP73-GFP (Fig. 5A and B). Meanwhile, CYCLOPS-GFP also colocalized with CCaMK-mCherry in the nucleus.

Concurrence of interactions of CIP73/CCaMK and CIP73/HIP in the same cell.

We took advantage of a multicolor BiFC system (Waadt et al. 2008) to investigate whether the interactions between CIP73 and CCaMK and between CIP73 and HIP could take place simultaneously in the same cell. For this observation, three *Agrobacterium tumefaciens* strains, each harboring an expression construct, were mixed and used to coinfiltrate *N. benthamiana* leaf cells. CIP73

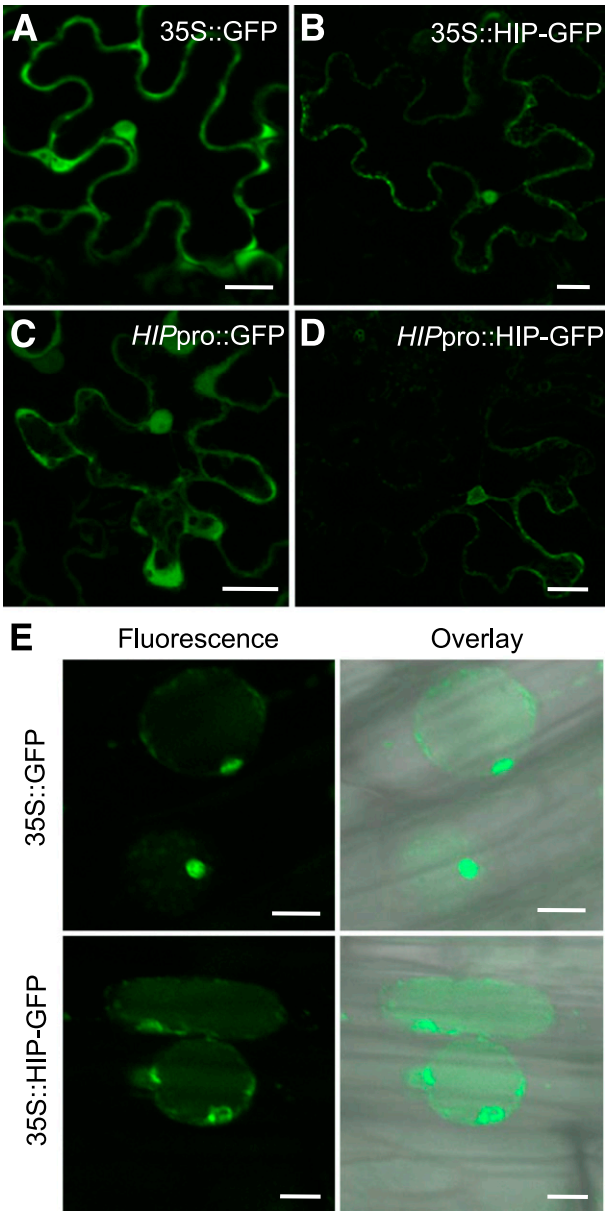

Fig. 4. Subcellular localization of HSC/HSP70 interacting protein (HIP) in *Nicotiana benthamiana* and *Lotus japonicus* cells. **A** to **D,** Localization of HIP in *N. benthamiana* leaf cells. HIP-green fluorescent protein (GFP) was expressed under the control of either the *Cauliflower mosaic virus* 35S promoter (B) or the *HIP* native promoter (D). GFP alone served as a control (A and C). **E,** Localization of GFP-tagged HIP under the control of the 35S promoter in *L. japonicus* hairy roots. The hairy roots were treated with 4% NaCl for 5 min before imaging. GFP alone served as a control. Green fluorescence (left) and brightfield images of the same cells were superimposed to produce the overlay images (right). Scale bars represent 20 μm.

was fused with the C-terminus of cyan fluorescent protein (CFPC-CIP73), CCaMK was fused with the N-terminus of CFP (CCaMK-CFPN), and HIP with the N-terminus of Venus (HIP-VenusN). Three days after infiltration, leaf cells were subjected to confocal laser-scanning microscopic examination. The interaction between CIP73 and HIP was detected as green fluorescence signal and the interaction between CIP73 and CCaMK was observed in red fluorescence (Fig. 5C). Both green and red fluorescence signals were detected in the nucleus of the same cells (Fig. 5C). Identical results were obtained when the split fluorescent tags were exchanged between CCaMK and HIP (Fig. 5D). These results suggest that both interactions between CIP73 and HIP and between CIP73 and CCaMK could concur in the same nucleus and a protein complex consisting of the three partners may exist in the nuclei.

Downregulated expression of *HIP* during nodulation.

To determine the temporal and spatial expression of the *HIP* gene, we examined the transcriptional expression patterns from the *Lotus japonicus* Gene Expression Atlas (LjGEA) (Verdier et al. 2013). *HIP* cDNA sequence identified two probe sets (chr4.CM0126.62_at and chr4.CM0126.62.1_at) on the Affymetrix *Lotus* Gene Chip. Analysis of the microarray data revealed that *HIP* is widely expressed in various tissues, including roots, nodules, stems, leaves, petiole, flowers, pods, and seeds. To confirm the *HIP* gene expression data, we took a real-time quantitative reverse transcription-polymerase chain reaction (qRT-PCR) approach to measure the transcript levels of *HIP* in different tissues and nodulation stages. *HIP* transcripts were detected at higher levels in both roots and shoots but at a very low level in nodules (Fig. 6B). After inoculation with *M. loti*, the transcript level of *HIP* was slightly elevated in roots 1 day postinoculation (dpi) and soon returned to its original level at 2 dpi. The expression level then dropped drastically between 8 and 25 dpi (Fig. 6A), indicating that *HIP* expression is down-regulated during nodule development and nodule senescence.

To analyze the spatial expression pattern of *HIP* at the cellular level, the *HIP* gene promoter was used to drive the expression of β-glucuronidase (GUS) reporter in transgenic hairy roots of *L. japonicus*. In noninoculated hairy roots, GUS activity was mainly detected in the root tip, vascular bundles, and

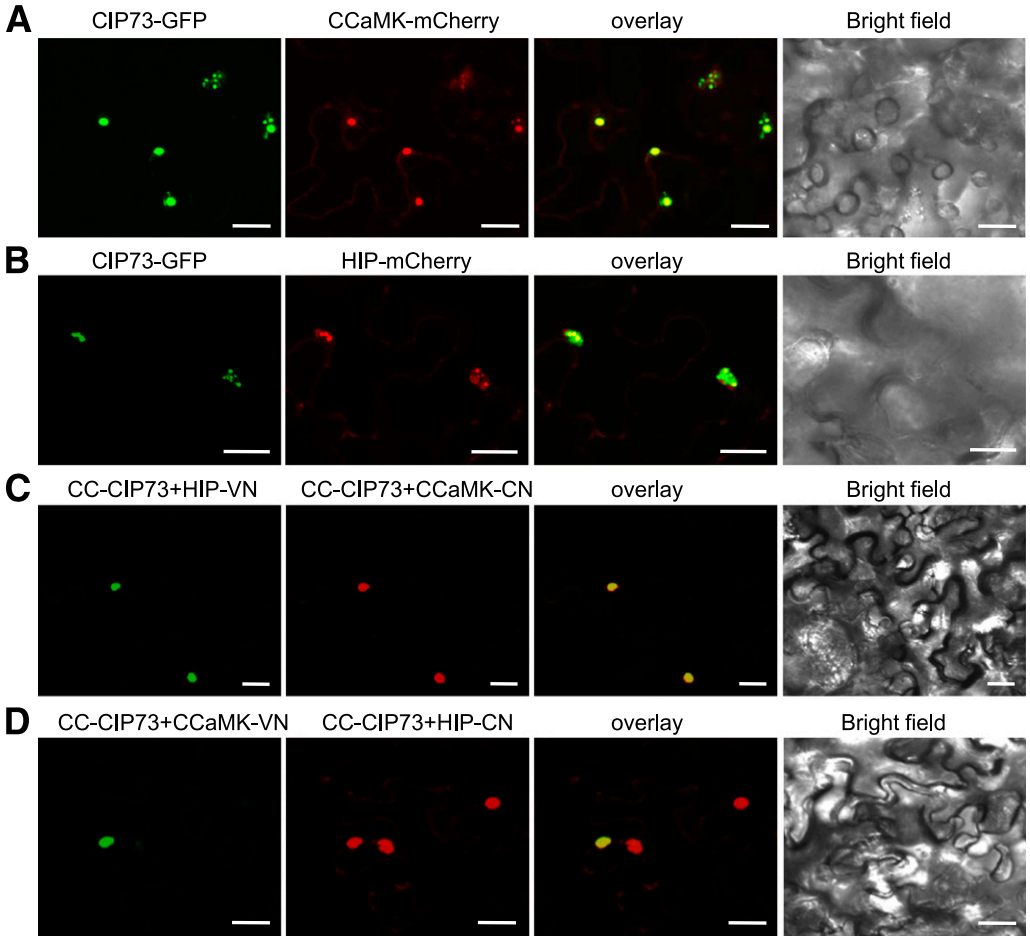

Fig. 5. Co-localization of CIP73, HSC/HSP70 interacting protein (HIP), and calcium and calmodulin-dependent protein kinase (CCaMK) and multicolor bimolecular fluorescence complementation (BiFC) analysis of subcellular sites of interactions. **A,** Coexpression of CIP73-GFP and CCaMK-mCherry in *Nicotiana benthamiana* leaf cells. CCaMK-mCherry (red) colocalized with CIP73-GFP (green) in the nuclei as shown by the yellow color in the overlay image. **B,** Coexpression of CIP73-GFP and HIP-mCherry in *N. benthamiana* leaf cells. HIP-mCherry (red) colocalized with CIP73-GFP (green) in the nuclei as shown by the yellow color in the overlay image. **C** and **D,** Multicolor BiFC analysis of concurrence of the interactions between CIP73 and HIP and between CIP73 and CCaMK in the same *N. benthamiana* leaf cells. CIP73 was expressed as a fusion protein with the C-terminal cyan fluorescent protein (CFP). HIP and CCaMK were fused with the N-terminal CFP and Venus, respectively. The interaction between CC-CIP73 and HIP-VN resulted in green fluorescence, whereas the interaction between CC-CIP73 and CCaMK-CN led to red fluorescence (C). Identical results were obtained when the fluorescent tags were exchanged between CCaMK and HIP (D). Fluorescent images of *N. benthamiana* epidermal leaf cells were taken using confocal laser scanning microscope 3 days postinfiltration with *Agrobacterium* cells harboring appropriate constructs. Overlay images were generated by superimposing green and red images. CC, C-terminal CFP; CN, N-terminal CFP; VN, N-terminal Venus. Scale bars represent 20 μm.

lateral root primordia (Fig. 6C and D). After inoculation with *M. loti*, the *HIP* promoter activity was observed at the nodule primordia (Fig. 6E) and was down-regulated drastically in fully matured nodules (Fig. 6F and G).

HIP plays a negative role during early nodulation.

To investigate the possible role of *HIP* in nodulation, we attempted to identify mutants of *L. japonicus HIP* from the LORE1 retrotransposon insertion population (Fukai et al. 2012; Urbański et al. 2012). One mutant line, 30002690, was identified with an insertion in the first intron of the *HIP* gene (Supplementary Fig. 7A and B). We determined the *HIP* mRNA levels in this mutant and did not find any difference in the *HIP* mRNA level between the mutant and the wild-type control. Apparently, the first intron containing the inserted retrotransposon was spliced out with no effect on the *HIP* mRNA level. We then examined the role of *HIP* in nodulation, using an RNAi approach in transgenic hairy roots. Two *HIP*-specific RNAi constructs were prepared to knockdown *HIP* expression by targeting the 438-bp 5′ region (RNAi-1) and the 299-bp 3′ region (RNAi-2) of the *HIP* gene transcript. We generated transgenic hairy roots expressing the two *HIP* RNAi constructs, and the empty vector was used as a control. The level of *HIP* transcripts in transgenic hairy roots was reduced to 22% in *HIP* RNAi-1 and 51% in *HIP* RNAi-2, on average, as compared with the control hairy roots (Fig. 7A). Transgenic hairy roots were inoculated with *M. loti*, and nodulation phenotypes were examined. At 16 dpi, the average number of nodules formed on control hairy roots was 4.5 (n = 62), while that on RNAi-1 and RNAi-2 hairy roots was increased to 7.6 (n = 63) and 6.1 (n = 65), respectively (Fig. 7B). This increase in nodule number by *HIP* RNAi expression was statistically significant ($P < 0.05$, t test). However, the difference was no longer significant at 32 dpi (Fig. 7B), indicating that RNAi-mediated knockdown of *HIP* expression could only promote nodulation at the early stage. The increased nodulation on RNAi hairy roots at 16 DPI suggests that HIP may play a negative regulatory role in the early stages of nodulation.

DISCUSSION

CCaMK is a Ca^{2+}-spiking decoder and a central regulator for both RNS and AMS. It has long been thought that NSP1, NSP2, and other transcription factors may act as direct targets of symbiosis signals downstream of CcaMK, in order to activate symbiosis-specific gene expression. However, no direct evidence has been presented to support this hypothesis. No transcription factor has been identified to be a direct phosphorylation target of

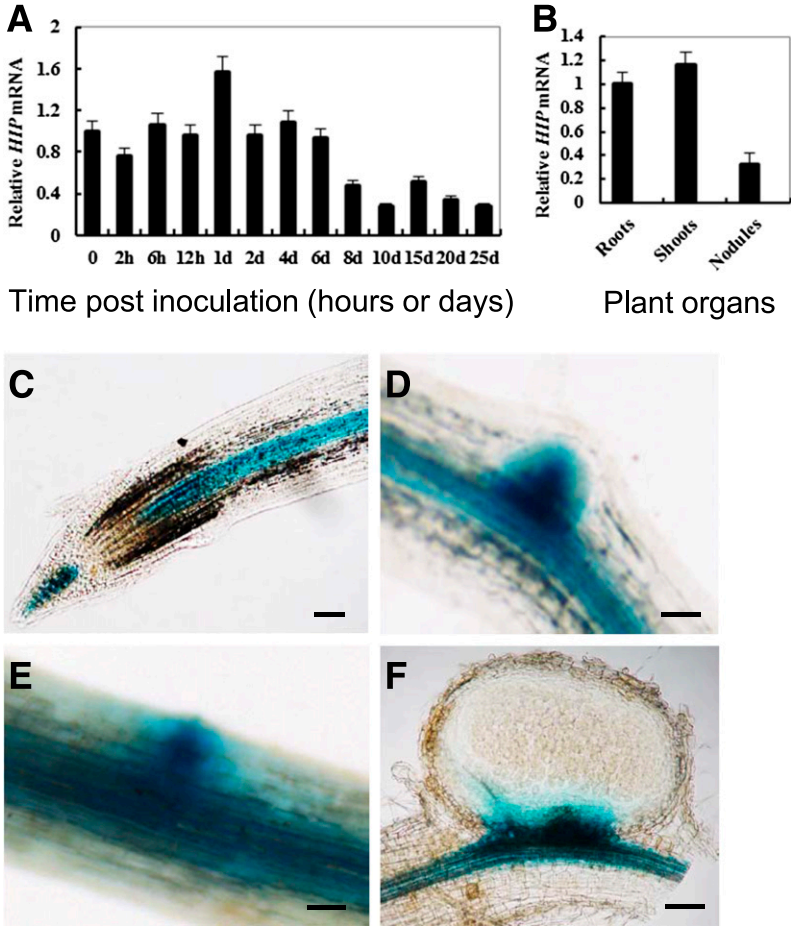

Fig. 6. Temporal and spatial expression patterns of *Lotus japonicus HIP*. **A,** *HIP* gene expression in infected roots. Total RNA samples were taken from roots at different time points postinoculation with *Mesorhizobium loti*. Relative *HIP* mRNA levels were quantified by quantitative reverse transcription-polymerase chain reaction using *ubiquitin* gene expression as an internal control. Noninoculated roots served as a control. Error bars indicate ± standard deviation. **B,** *HIP* expression in different *L. japonicus* tissues. Total RNA samples were taken from *Rhizobium*-inoculated roots, shoots, and nodules 15 days postinoculation with *M. loti*. **C** through **F,** Histochemical analysis of *HIP*pro::GUS expression in roots and nodules. A 1.6-kb *L. japonicus HIP* native promoter was used to drive GUS reporter expression in transgenic hairy roots of *L. japonicus*. The *HIP* promoter activity was observed in the root tip, vascular bundle (C), and lateral root primordia (D) of noninoculated roots, and in the nodule primordia (E). Note that *HIP* promoter activity became weaker in matured nodules (F). The nodules were harvested for sectioning 21 days after inoculation with rhizobia. Scale bars represent 100 μm.

CCaMK. On the other hand, two novel proteins with unknown functions, CYCLOPS and CIP73, have been found to be direct phosphorylation targets of CCaMK (Kang et al. 2011; Yano et al. 2008). Moreover, the molecular mechanisms underlying the regulation of CCaMK and signal relay between CCaMK, CYCLOPS, and CIP73 have yet to be elucidated. In this report, we identified HIP as an interacting partner of CIP73 and show that CIP73 may serve as a scaffold that brings HIP and CCaMK together to form a protein complex in the nuclei.

HIP is a conserved protein in eukaryotes.

HIP homologs are widely present in eukaryotes, including protists, animals, and plants (Fig. 1B) but are absent in prokaryotes, suggesting that HIP proteins may play roles that are unique to eukaryotic cells. Animal HIP has been shown to facilitate the chaperone function of HSC/HSP70 in protein folding and repair and in controlling the assembly of steroid receptors and the activity of regulators of cell proliferation and apoptosis (Caruso and Reiners 2006; Li et al. 2013; Nollen et al. 2000). Although the bioinformatics data of an *Arabidopsis* HIP homolog has been reported (Webb et al. 2001), the biological function of HIP proteins in plants have not been characterized. In this work, HIP was linked to the symbiosis signaling pathway via interaction with CIP73. Contrary to HIP, both CIP73 and CCaMK proteins appear to be unique to plants, although the Scythe_N ubiquitin-like domain in CIP73 and the N-terminal protein kinase domain and CaM-binding domain in CCaMK share significant homology with animal proteins (Kang et al. 2011; Harper et al. 2004).

HIP is present in both the cytoplasm and nucleus.

In animal cells, HIP was first identified as a cytoplasmic homo-oligomeric protein (Höhfeld et al. 1995). Further studies on HIP have demonstrated that animal HIP is the 48-kDa component (p48) of the progesterone receptor-chaperone complexes and may shuttle between the cytoplasm and nucleus (Prapapanich et al. 1996b). Consistent with this, our results showed that *L. japonicus* HIP is distributed in both the cytoplasm and nucleus (Fig. 4) and may interact with CIP73 in both subcellular locations (Fig. 3). Previous studies have shown that DMI3/CCaMK is localized exclusively in the nucleus of root-hair cells and epidermal root cells in *M. truncatula* (Kaló et al. 2005; Smit et al. 2005). However, our data showed that *L. japonicus* CCaMK is localized in both the cytoplasm and nucleus. Expression of the kinase domain of *L. japonicus* CCaMK in *N. benthamiana* leaf epidermal cells has been shown to target the protein to both the cytoplasm and nucleus (Takeda et al. 2012). Recombinant rice CCaMK has also been shown to distribute in the nucleus, cytoplasm, and plasma membrane when expressed in rice protoplasts (Shi et al. 2012). The occurrence and function of CCaMK in the cytoplasm and nucleus warrant further investigation in future studies.

A potential protein complex consisting of CIP73, CcaMK, and HIP.

Unlike HIP, CIP73 is localized exclusively in the nucleus (Kang et al. 2011). Moreover, the nuclear localization of CCaMK has been found to be important for its functions in AMS and RNS (Takeda et al. 2012). Our analysis using BiFC revealed that CIP73 interacts with HIP in both the cytoplasm and nucleus (Fig. 3). In order to test whether CIP73, HIP, and CCaMK could colocalize in the nucleus and whether coexpression of these three proteins might alter the subcellular localization patterns of each protein, we examined *N. benthamiana* leaf cells expressing recombinant proteins tagged with fluorescent proteins. HIP was colocalized with CCaMK and CIP73 in the nuclei, and the cytoplasmic distribution of HIP was reduced when coexpressed with CIP73 (Fig. 5 A and B). Because both HIP and CCaMK could interact with CIP73, we investigated whether the interactions between CIP73 and CCaMK and between CIP73 and HIP could take place concurrently in the same cells. Using the multicolor BiFC approach, we conclude that these protein-protein interactions could, indeed, take place simultaneously in the nuclei of same cells (Fig. 5 C and D). This result implies that a protein complex consisting of CIP73, CcaMK, and HIP may exist in the nuclei.

A negative regulator of nodulation.

Animal HIP is also known as ST13 (suppression of tumorigenicity 13), a downregulated protein in colorectal cancers (Shi et al. 2007). Short hairpin RNA–mediated downregulation of ST13 has been found to significantly increase cell proliferation and tumorigenicity (Bai et al. 2012). The striking protein similarity of *L. japonicus* HIP to ST13 supports the idea that *L. japonicus* HIP may play a similar role in regulation of cell proliferation in plants. Consistent with this notion, the expression of *L. japonicus HIP* was found to be downregulated during the nodulation process and in mature nodules (Fig. 6). RNAi-mediated knockdown of *L. japonicus HIP* expression in transgenic hairy roots led to increased nodule formation at early

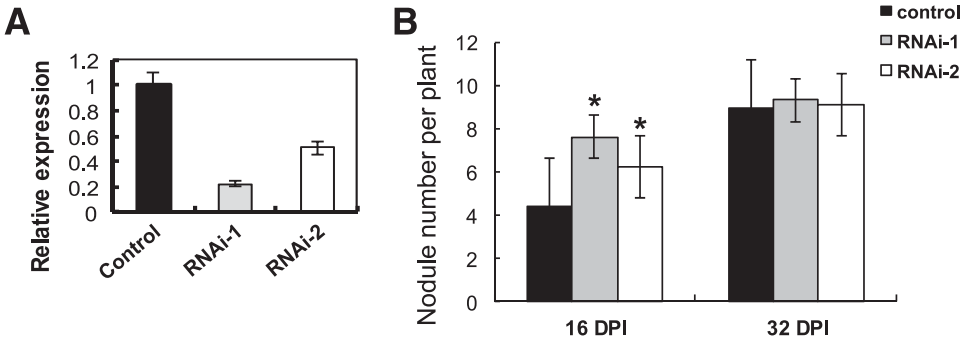

Fig. 7. Nodulation phenotypes of transgenic hairy roots of *Lotus japonicus* expressing HSC/HSP70 interacting protein gene (*HIP*)-specific RNAi. **A,** Analysis of relative *HIP* transcript levels by quantitative reverse transcription-polymerase chain reaction (qRT-PCR). Total RNA was isolated from representatives of transgenic hairy roots expressing *HIP* RNAi-1 and RNAi-2 constructs, and relative *HIP* transcript levels were quantified by qRT-PCR, using *Ubiquitin* gene expression as an internal control. Hairy roots expressing the empty vector served as a control. Error bars indicate ± standard deviation for six independent transformants per line and three technical replicates. **B,** Total numbers of nodules per plant on transgenic hairy roots expressing the empty vector (control), *HIP* RNAi-1, and RNAi-2 at 16 and 32 days postinoculation (DPI), respectively. Asterisks above the bars indicate statistically significant differences ($P < 0.05$, *t* test) between the control and *HIP* RNAi-1 or RNAi-2. Note that the difference was no longer significant at 32 days postinoculation. Error bars represent the standard deviation.

nodulation stages (Fig. 7). These data suggest that *L. japonicus* HIP may play a negative regulatory role in nodulation by serving as a repressor of cell proliferation similar to the role of ST13 in cancer cells.

Search for other cochaperones for HIP.

L. japonicus HIP protein contains multiple functional domains, including a conserved N-terminal dimerization domain, a central TPR domain flanked by highly charged regions, a stretch of degenerate GGMP repeats, and a C-terminal domain similar to the STI1/HOP/p60 protein (Irmer and Höhfeld 1997; Prapapanich et al. 1996a). Compared with the animal HIPs, plant HIPs have an expanded region of GGMP repeats. The animal HIP has been well characterized with regard to interaction with HSC/HSP70 and other cochaperones (Demand et al. 1998; Höhfeld et al. 1995), but whether *L. japonicus* HIP interacts with HSC/HSP70 and other cochaperones is not known. The TPR domain and its flanking charged regions of animal HIP proteins are known to be required for binding with the ATPase domain of HSC/HSP70 (Liu et al. 1999). It remains to be tested whether the N-terminal TPR domain and GGMP motif of *L. japonicus* HIP interact with *L. japonicus* HSC/HSP70. Our results show that the C-terminal STI1-like domain of *L. japonicus* HIP is necessary and sufficient for the interaction with CIP73 (Fig. 2). The yeast ortholog of animal STI1 is cochaperone HOP/p60, which mediates organization of HSP70 and HSP90 in multichaperone heterocomplexes (Carrigan et al. 2004; Smith et al. 1993). The TPR domain is also present in yeast HOP/p60 and animal HSP90-binding immunophilins (Owens-Grillo et al. 1996; Smith et al. 1993). HSC/HSP70 represents a large molecular chaperone family composed of both the constitutively expressed 70-kDa heat-shock cognate protein HSC70 and the heat-inducible HSP70 (Boorstein et al. 1994). HSC/HSP70 proteins are ubiquitous and conserved in both animals and plants. Members of the HSC/HSP70 family in plants have been found in multiple subcellular compartments, including the nucleus, cytoplasm, mitochondria, endoplasmic reticulum, chloroplast, and peroxisome (Boston et al. 1996; Miernyk 1999), but their functions are not well-known. Whether *L. japonicus* HIP interacts with HSC/HSP70 and other cochaperones in *L. japonicus*, as in animals, remains to be investigated.

In conclusion, the identification of HIP as an interacting partner of CIP73 revealed possible involvement of HIP in CCaMK-mediated Ca^{2+} decoding and symbiosis signaling during nodule development. CIP73 may act as a scaffold for the formation of a HIP-CIP73-CCaMK protein complex that may exert its biochemical function in the nuclei. As a negative regulator of nodulation, HIP may prove to be an important player in regulating cell proliferation required for nodule organogenesis.

MATERIALS AND METHODS

Plant materials and growth conditions.

Seeds of *L. japonicus* MG-20 Miyakojima were surface-sterilized in 75% ethanol for 2 min and, then, in 2% sodium hypochlorite for 8 min, followed by washing seven times with sterile water. The seeds were left to germinate for 48 h at 22°C on sterile water-soaked filter paper in petri dishes in the dark. Seedlings were subsequently planted in pots filled with sand and vermiculite (1:1 vol/vol) supplemented with half-strength nitrogen-free Broughton & Dilworth medium and were grown in a growth chamber maintained at 22 ± 1°C with a 16-h-day and 8-h-night cycle. Five-day-old seedlings were inoculated with *Mesorhizobium loti* MAFF303099. *Nicotiana benthamiana* plants were grown in nutrient soil in growth chambers with a 16-h-light and 8-h-dark cycle at 26°C for about 1 to 1.5 months before infiltration with *Agrobacterium tumefaciens*. After infiltration, plants were maintained under the same growth conditions.

Yeast two-hybrid screening.

A cDNA fragment encoding the C-terminal region of CIP73 (414 to 691 amino acids), which did not have autoactivation in yeast cells, was fused in-frame with the GAL4 DNA-binding domain in pGBKT7 vector. Bait constructs were transformed into yeast strain Y187 by the lithium acetate method. Screening of a *L. japonicus* root cDNA library constructed in prey vector (Zhu et al. 2008) was carried out via mating, according to the manufacturer's instructions (Clontech). For testing protein-protein interactions, a bait construct plasmid and a prey construct plasmid were transformed into yeast strains Y187 and AH109, respectively. After mating of the two yeast strains, colonies grew on SD/-Trp/-Leu plates were transferred to SD/-Trp/-Leu/X-gal and SD/-Trp/-Leu/-His/-Ade/X-gal plates for evaluation of protein-protein interactions.

Phylogenetic analysis and sequence alignment.

HIP proteins were aligned using ClustalX version 1.83 (Kim and Joo 2010) and an unrooted tree was generated with the neighbor-joining method (Saitou and Nei 1987) and bootstrap analysis (1000 replicates). The tree was analyzed and displayed using MEGA software version 5 (Tamura et al. 2011).

In vitro protein-protein interaction.

To assay the interaction between CIP73 and HIP in vitro, CBD-tagged HIP was bound to chitin beads (New England Biolabs). The beads were incubated with 2 μg of purified His-CIP73 protein in 1 ml of interaction buffer (20 mM Tris-HCl, 100 mM NaCl, 50 mM KCl, 0.5 mM EDTA, 1 mM $MgCl_2$, and 5% glycerol, pH 8.0). The reaction was incubated for 1 h on ice with gentle shaking. The chitin beads were collected and were washed five times in 1 ml of interaction buffer. The retained proteins were eluted by boiling for 5 min in 1× SDS sample buffer and were separated by SDS-PAGE. Subsequent immunoblotting of pulled-down proteins was carried out with the anti-His-tag antibody or visualized by staining with Coomassie brilliant blue. His-tagged CIP73 were purified using nickel-agarose beads (Qiagen).

Tobacco leaf infiltration and multicolor BiFC analysis.

The full-length coding region of *CIP73* was PCR-amplified and was cloned into the *Spe*I/*Sal*I site of pSCYCE-R vector (Waadt et al. 2008) to obtain the CIP73-CC fusion. The full-length coding regions of *HIP* and *CCaMK* without the stop codon were cloned into the *Bam*HI/*Sma*I site or the *Spe*I/*Sma*I sites of pSCYNE, respectively, to obtain the HIP-VN and CCaMK-CN or HIP-CN and CCaMK-VN fusions. The constructs were transferred into *A. tumefaciens* GV3101/PMP90 or EHA105 by electroporation. Fresh *Agrobacterium* cells containing proper plasmids were grown in Luria Bertani (LB) medium at 28°C in a shaker for 24 h. The cells were transferred to fresh LB medium (1:100 ratio, vol/vol) containing 10 mM 2-(N-morpholine)-ethanesulfonic acid (MES) (pH 5.6) and 40 μM acetosyringone (AS). After 16 h of growth at 28°C, the bacterial cells were spun down gently at 5,000 × *g* for 5 min. The pellet was resuspended in infiltration buffer (10 mM $MgCl_2$, 10 mM MES-KOH, 200 μM AS) at a final optical density at 600 nm (OD_{600}) of 1.5. For *Agrobacterium* sp. strain p19, a final OD_{600} of 1.0 was used instead. The cells were incubated on bench for 2 to 4 h at room temperature before infiltration. For coinfiltration, an equal volume of different *Agrobacterium* strains carrying plasmids was mixed together prior to infiltration. The bacteria mixture was infiltrated into the top leaves of 6-week-old *Nicotiana benthamiana* with a 1- to 2-ml syringe. Fluorescence of

leaf cells was assayed 2 to 3 days after infiltration using an Olympus FV1000 laser scanning microscope.

Subcellular localization of CIP73, HIP, and CCaMK.

Two expression vectors, pCAMBIA1301-eGFP and pCAMBIA1301-mCherry, were constructed for subcellular localization and colocalization studies. The cDNA encoding eGFP (enhanced green fluorescent protein) (Clontech) with the nopaline synthase terminator was placed behind the enhanced CaMV 35S promoter. The whole expression unit was then cloned to the *Hin*dIII/*Eco*RI site of pCAMBIA1301 to generate pCAMBIA1301-eGFP, which eliminated the multiple cloning sites of pCAMBIA1301 and introduced new multiple cloning sites in front of eGFP. The eGFP coding region was replaced by the mCherry coding region to generate pCAMBIA1301-mCherry. For expression of the tagged protein under the control of the *HIP* gene promoter, the CaMV 35S promoter in the two vectors was replaced by the *HIP* gene promoter.

The *CIP73*, *HIP*, and *CCaMK* cDNAs without the stop codon were cloned into the corresponding cloning sites of pCAMBIA1301-eGFP or pCAMBIA1301-mCherry to obtain CIP73-eGFP, HIP-eGFP, and CCaMK-eGFP or CIP73-mCherry, HIP-mCherry, and CCaMK-mCherry fusions. These constructs were transferred into *Agrobacterium rhizogenes* LBA1334 for *Lotus japonicus* hairy root transformation or *A. tumefaciens* EHA105 for *N. benthamiana* transformation. Fluorescence signals of transgenic cells were examined using an Olympus FV1000 laser scanning microscope.

Hairy-root transformation and GUS-staining assays.

Hairy root transformation of *L. japonicus* MG20 using *A. rhizogenes* LBA1334 was performed as described previously (Kang et al. 2011). The hygromycin gene in vector pC1302 was substituted by the *GUS* gene to generate pCAMBIA1302GUS vector. The *GUS* gene in vectors pCAMBIA1301 and pCAMBIA1302GUS was used for selection of transgenic hairy roots. For selection of transformed hairy roots, a root tip of hairy roots was removed and was incubated in GUS staining solution (100 mM sodium phosphate buffer, pH 7.0, 0.1% Triton X-100, 0.1% N-laurylsarcosine, 10 mM Na_2EDTA, 1 mM $K_3Fe(CN)_6$, 1 mM $K_4Fe(CN)_6$, and 0.5 mg ml^{-1} 5-bromo-4-chloro-3-indolyl-D-glucuronic acid [X-Gluc] [Sigma]) overnight at 37°C in the dark. GUS-positive hairy roots were allowed to continue to grow and were used for further analysis.

Gene expression analysis.

Expression profile of the *HIP* gene was analyzed by qRT-PCR. Total RNAs were isolated from *L. japonicus* plants using Trizol reagent (Invitrogen). The amount of total RNA was normalized by measuring the RNA concentration at 260 nm using a NanoDrop 2000 (Thermo) apparatus according to manufacturer's instructions. The Primescript RT reagent kit (Takara) was used to eliminate genomic DNA contamination and to synthesize first-strand cDNA. Real-time RT-PCR was performed using the SYBR Select master mix (ABI). PCR reactions were carried out using the standard cycling mode: 2 min at 50°C for UDG activation, 2 min at 95°C, followed by 40 cycles of 15 s at 95°C and 1 min at 60°C. Expression levels were normalized using *Ubiquitin* (AW720576) as an internal control. Three independent biological replicates were performed for each condition tested.

***HIP* promoter-GUS construction.**

For HIP_{Pro}:GUS reporter analysis, a 1.6-kb genomic DNA upstream of the *HIP* coding region was amplified by PCR using primers 5′-AACTGCAGCACTTCTCATATTTTAACCG-3′ and 5′-ATCGGATCCGTTTTGGTCTGTGAAAGC-3′. The promoter was cloned into the *Pst*I/*Bam*HI site upstream of the GUS gene in the binary vector of pCAMBIA1391Z. Transgenic hairy roots of *L. japonicus* expressing HIP_{Pro}:GUS were incubated with X-Gluc solution. GUS activity of hairy roots without rhizobial inoculation served as a control. To make sections, stained nodules were embedded into 3% agarose and were sliced into 200-µm-thick sections using a vibratome (Leica VT1200).

Knockdown of *HIP* by RNAi.

For *HIP* knockdown analyses, a 438-bp 5′ region (RNAi-1) and a 299-bp 3′ region (RNAi-2) of the *HIP* transcript were amplified by PCR from *L. japonicus* cDNA. The forward primers contained *Pst*I-*Sma*I sites and the reverse primers had *Sal*I-*Bam*HI sites. Amplified cDNA products were digested and ligated into the *Sma*I/*Bam*HI site and, then, the *Pst*I/*Sal*I site of pCAMBIA1301-35S-int-T7 vector. The resulting construct contained a sense and an antisense *HIP* cDNA sequence, which was interrupted by the *Arabidopsis actin-11* intron. This intron-hairpin RNA construct was placed behind the CaMV 35S promoter. The RNAi binary vector was transferred into *A. rhizogenes* LBA1334 by electroporation for *L. japonicus* hairy root transformation. Analysis of root growth and nodulation phenotypes was performed as described previously (Kang et al. 2014).

ACKNOWLEDGMENTS

This work was supported by the National Natural Science Foundation of China (grant number 31200188), the China Postdoctoral Science Foundation (grant number 2012M521436 and 2013T60727), and Huazhong Agricultural University Scientific and Technological Self-Innovation Foundation (Program number 2662014BQ016).

LITERATURE CITED

Bai, R., Shi, Z., Zhang, J. W., Li, D., Zhu, Y. L., and Zheng, S. 2012. ST13, a proliferation regulator, inhibits growth and migration of colorectal cancer cell lines. J. Zhejiang Univ. Sci. B 13:884-893.

Boorstein, W. R., Ziegelhoffer, T., and Craig, E. A. 1994. Molecular evolution of the HSP70 multigene family. J. Mol. Evol. 38:1-17.

Boston, R. S., Viitanen, P. V., and Vierling, E. 1996. Molecular chaperones and protein folding in plants. Plant Mol. Biol. 32:191-222.

Capoen, W., Den Herder, J., Sun, J., Verplancke, C., De Keyser, A., De Rycke, R., Goormachtig, S., Oldroyd, G., and Holsters, M. 2009. Calcium spiking patterns and the role of the calcium/calmodulin-dependent kinase CCaMK in lateral root base nodulation of *Sesbania rostrata*. Plant Cell 21:1526-1540.

Capoen, W., Sun, J., Wysham, D., Otegui, M. S., Venkateshwaran, M., Hirsch, S., Miwa, H., Downie, J. A., Morris, R. J., Ané, J. M., and Oldroyd, G. E. 2011. Nuclear membranes control symbiotic calcium signaling of legumes. Proc. Natl. Acad. Sci. U.S.A. 108:14348-14353.

Carrello, A., Allan, R. K., Morgan, S. L., Owen, B. A., Mok, D., Ward, B. K., Minchin, R. F., Toft, D. O., and Ratajczak, T. 2004. Interaction of the Hsp90 cochaperone cyclophilin 40 with Hsc70. Cell Stress Chaperones 9:167-181.

Carrigan, P. E., Nelson, G. M., Roberts, P. J., Stoffer, J., Riggs, D. L., and Smith, D. F. 2004. Multiple domains of the co-chaperone Hop are important for Hsp70 binding. J. Biol. Chem. 279:16185-16193.

Caruso, J. A., and Reiners, J. J., Jr. 2006. Proteolysis of HIP during apoptosis occurs within a region similar to the BID loop. Apoptosis 11: 1877-1885.

Chen, C., Gao, M., Liu, J., and Zhu, H. 2007. Fungal symbiosis in rice requires an ortholog of a legume common symbiosis gene encoding a Ca^{2+}/calmodulin-dependent protein kinase. Plant Physiol. 145:1619-1628.

De Koninck, P., and Schulman, H. 1998. Sensitivity of CaM kinase II to the frequency of Ca^{2+} oscillations. Science 279:227-230.

Demand, J., Lüders, J., and Höhfeld, J. 1998. The carboxy-terminal domain of Hsc70 provides binding sites for a distinct set of chaperone cofactors. Mol. Cell. Biol. 18:2023-2028.

Fukai, E., Soyano, T., Umehara, Y., Nakayama, S., Hirakawa, H., Tabata, S., Sato, S., and Hayashi, M. 2012. Establishment of a Lotus japonicus gene tagging population using the exon-targeting endogenous retrotransposon LORE1. Plant J. 69:720-730.

Gleason, C., Chaudhuri, S., Yang, T., Muñoz, A., Poovaiah, B. W., and Oldroyd, G. E. 2006. Nodulation independent of rhizobia induced by a calcium-activated kinase lacking autoinhibition. Nature 441:1149-1152.

Godfroy, O., Debellé, F., Timmers, T., and Rosenberg, C. 2006. A rice calcium- and calmodulin-dependent protein kinase restores nodulation to a legume mutant. Mol. Plant-Microbe Interact. 19:495-501.
Harper, J. F., and Harmon, A. 2005. Plants, symbiosis and parasites: A calcium signalling connection. Nat. Rev. Mol. Cell Biol. 6:555-566.
Harper, J. F., Breton, G., and Harmon, A. 2004. Decoding Ca^{2+} signals through plant protein kinases. Annu. Rev. Plant Biol. 55:263-288.
Hayashi, T., Banba, M., Shimoda, Y., Kouchi, H., Hayashi, M., and Imaizumi-Anraku, H. 2010. A dominant function of CCaMK in intracellular accommodation of bacterial and fungal endosymbionts. Plant J. 63:141-154.
Hernández Torres, J., Papandreou, N., and Chomilier, J. 2009. Sequence analyses reveal that a TPR-DP module, surrounded by recombinable flanking introns, could be at the origin of eukaryotic Hop and Hip TPR-DP domains and prokaryotic GerD proteins. Cell Stress Chaperones 14, 3:281-289.
Höhfeld, J., Minami, Y., and Hartl, F. U. 1995. Hip, a novel cochaperone involved in the eukaryotic Hsc70/Hsp40 reaction cycle. Cell 83:589-598.
Horváth, B., Yeun, L. H., Domonkos, A., Halász, G., Gobbato, E., Ayaydin, F., Miró, K., Hirsch, S., Sun, J., Tadege, M., Ratet, P., Mysore, K. S., Ané, J. M., Oldroyd, G. E., and Kaló, P. 2011. *Medicago truncatula* IPD3 is a member of the common symbiotic signaling pathway required for rhizobial and mycorrhizal symbioses. Interact. 24:1345-1358.
Irmer, H., and Höhfeld, J. 1997. Characterization of functional domains of the eukaryotic co-chaperone Hip. J. Biol. Chem. 272:2230-2235.
Kaló, P., Gleason, C., Edwards, A., Marsh, J., Mitra, R. M., Hirsch, S., Jakab, J., Sims, S., Long, S. R., Rogers, J., Kiss, G. B., Downie, J. A., and Oldroyd, G. E. 2005. Nodulation signaling in legumes requires NSP2, a member of the GRAS family of transcriptional regulators. Science 308: 1786-1789.
Kang, H., Zhu, H., Chu, X., Yang, Z., Yuan, S., Yu, D., Wang, C., Hong, Z., and Zhang, Z. 2011. A novel interaction between CCaMK and a protein containing the Scythe_N ubiquitin-like domain in *Lotus japonicus*. Plant Physiol. 155:1312-1324.
Kang, H., Chu, X., Wang, C., Xiao, A., Zhu, H., Yuan, S., Yang, Z., Ke, D., Xiao, S., Hong, Z., and Zhang, Z. 2014. A MYB coiled-coil transcription factor interacts with NSP2 and is involved in nodulation in *Lotus japonicus*. New Phytol. 201:837-849.
Kim, T., and Joo, H. 2010. ClustalXeed: A GUI-based grid computation version for high performance and terabyte size multiple sequence alignment. BMC Bioinformatics 11:467.
Lefebvre, B., Timmers, T., Mbengue, M., Moreau, S., Hervé, C., Tóth, K., Bittencourt-Silvestre, J., Klaus, D., Deslandes, L., Godiard, L., Murray, J. D., Udvardi, M. K., Raffaele, S., Mongrand, S., Cullimore, J., Gamas, P., Niebel, A., and Ott, T. 2010. A remorin protein interacts with symbiotic receptors and regulates bacterial infection. Proc. Natl. Acad. Sci. U.S.A. 107:2343-2348.
Lévy, J., Bres, C., Geurts, R., Chalhoub, B., Kulikova, O., Duc, G., Journet, E. P., Ané, J. M., Lauber, E., Bisseling, T., Dénarié, J., Rosenberg, C., and Debellé, F. 2004. A putative Ca^{2+} and calmodulin-dependent protein kinase required for bacterial and fungal symbioses. Science 303: 1361-1364.
Li, Z., Hartl, F. U., and Bracher, A. 2013. Structure and function of Hip, an attenuator of the Hsp70 chaperone cycle. Nat. Struct. Mol. Biol. 20: 929-935.
Liao, J., Singh, S., Hossain, M. S., Andersen, S. U., Ross, L., Bonetta, D., Zhou, Y., Sato, S., Tabata, S., Stougaard, J., Szczyglowski, K., and Parniske, M. 2012. Negative regulation of CCaMK is essential for symbiotic infection. Plant J. 72:572-584.
Liu, F. H., Wu, S. J., Hu, S. M., Hsiao, C. D., and Wang, C. 1999. Specific interaction of the 70-kDa heat shock cognate protein with the tetratricopeptide repeats. J. Biol. Chem. 274:34425-34432.
Madsen, L. H., Tirichine, L., Jurkiewicz, A., Sullivan, J. T., Heckmann, A. B., Bek, A. S., Ronson, C. W., James, E. K., and Stougaard, J. 2010. The molecular network governing nodule organogenesis and infection in the model legume *Lotus japonicus*. Nat. Commun. 1:1-12.
Messinese, E., Mun, J. H., Yeun, L. H., Jayaraman, D., Rougé, P., Barre, A., Lougnon, G., Schornack, S., Bono, J. J., Cook, D. R., and Ané, J. M. 2007. A novel nuclear protein interacts with the symbiotic DMI3 calcium- and calmodulin-dependent protein kinase of *Medicago truncatula*. Mol. Plant-Microbe Interact. 20:912-921.
Miernyk, J. A. 1999. Protein folding in the plant cell. Plant Physiol. 121: 695-703.
Miller, J. B., Pratap, A., Miyahara, A., Zhou, L., Bornemann, S., Morris, R. J., and Oldroyd, G. E. 2013. Calcium/calmodulin-dependent protein kinase is negatively and positively regulated by calcium, providing a mechanism for decoding calcium responses during symbiosis signaling. Plant Cell 25:5053-5066.
Miwa, H., Sun, J., Oldroyd, G. E., and Downie, J. A. 2006. Analysis of calcium spiking using a cameleon calcium sensor reveals that nodulation gene expression is regulated by calcium spike number and the developmental status of the cell. Plant J. 48:883-894.
Nollen, E. A., Brunsting, J. F., Song, J., Kampinga, H. H., and Morimoto, R. I. 2000. Bag1 functions in vivo as a negative regulator of Hsp70 chaperone activity. Mol. Cell. Biol. 20:1083-1088.
Oldroyd, G. E. 2013. Speak, friend, and enter: Signalling systems that promote beneficial symbiotic associations in plants. Nat. Rev. Microbiol. 11:252-263.
Ovchinnikova, E., Journet, E. P., Chabaud, M., Cosson, V., Ratet, P., Duc, G., Fedorova, E., Liu, W., den Camp, R. O., Zhukov, V., Tikhonovich, I., Borisov, A., Bisseling, T., and Limpens, E. 2011. IPD3 controls the formation of nitrogen-fixing symbiosomes in pea and *Medicago Spp*. Interact. 24:1333-1344.
Owens-Grillo, J. K., Stancato, L. F., Hoffmann, K., Pratt, W. B., and Krishna, P. 1996. Binding of immunophilins to the 90 kDa heat shock protein (hsp90) via a tetratricopeptide repeat domain is a conserved protein interaction in plants. Biochemistry 35:15249-15255.
Poovaiah, B. W., Xia, M., Liu, Z., Wang, W., Yang, T., Sathyanarayanan, P. V., and Franceschi, V. R. 1999. Developmental regulation of the gene for chimeric calcium/calmodulin-dependent protein kinase in anthers. Planta 209:161-171.
Prapapanich, V., Chen, S., Toran, E. J., Rimerman, R. A., and Smith, D. F. 1996a. Mutational analysis of the hsp70-interacting protein Hip. Mol. Cell. Biol. 16:6200-6207.
Prapapanich, V., Chen, S., Nair, S. C., Rimerman, R. A., and Smith, D. F. 1996b. Molecular cloning of human p48, a transient component of progesterone receptor complexes and an Hsp70-binding protein. Mol. Endocrinol. 10:420-431.
Ramachandiran, S., Takezawa, D., Wang, W., and Poovaiah, B. W. 1997. Functional domains of plant chimeric calcium/calmodulin-dependent protein kinase: Regulation by autoinhibitory and visinin-like domains. J. Biochem. 121:984-990.
Routray, P., Miller, J. B., Du, L., Oldroyd, G., and Poovaiah, B. W. 2013. Phosphorylation of S344 in the calmodulin-binding domain negatively affects CCaMK function during bacterial and fungal symbioses. Plant J. 76:287-296.
Saitou, N., and Nei, M. 1987. The neighbor-joining method: A new method for reconstructing phylogenetic trees. Mol. Biol. Evol. 4:406-425.
Sathyanarayanan, P. V., Siems, W. F., Jones, J. P., and Poovaiah, B. W. 2001. Calcium-stimulated autophosphorylation site of plant chimeric calcium/calmodulin-dependent protein kinase. J. Biol. Chem. 276:32940-32947.
Shi, Z. Z., Zhang, J. W., and Zheng, S. 2007. What we know about ST13, a co-factor of heat shock protein, or a tumor suppressor? J. Zhejiang Univ. Sci. B 8:170-176.
Shi, B., Ni, L., Zhang, A., Cao, J., Zhang, H., Qin, T., Tan, M., Zhang, J., and Jiang, M. 2012. OsDMI3 is a novel component of abscisic acid signaling in the induction of antioxidant defense in leaves of rice. Mol. Plant 5:1359-1374.
Shimoda, Y., Han, L., Yamazaki, T., Suzuki, R., Hayashi, M., and Imaizumi-Anraku, H. 2012. Rhizobial and fungal symbioses show different requirements for calmodulin binding to calcium calmodulin-dependent protein kinase in *Lotus japonicus*. Plant Cell 24:304-321.
Smit, P., Raedts, J., Portyanko, V., Debellé, F., Gough, C., Bisseling, T., and Geurts, R. 2005. NSP1 of the GRAS protein family is essential for rhizobial Nod factor-induced transcription. Science 308:1789-1791.
Smith, D. F. 1993. Dynamics of heat shock protein 90-progesterone receptor binding and the disactivation loop model for steroid receptor complexes. Mol. Endocrinol. 7:1418-1429.
Smith, D. F., Sullivan, W. P., Marion, T. N., Zaitsu, K., Madden, B., McCormick, D. J., and Toft, D. O. 1993. Identification of a 60-kilodalton stress-related protein, p60, which interacts with hsp90 and hsp70. Mol. Cell. Biol. 13:869-876.
Takeda, N., Maekawa, T., and Hayashi, M. 2012. Nuclear-localized and deregulated calcium- and calmodulin-dependent protein kinase activates rhizobial and mycorrhizal responses in Lotus japonicus. Plant Cell 24: 810-822.
Takezawa, D., Ramachandiran, S., Paranjape, V., and Poovaiah, B. W. 1996. Dual regulation of a chimeric plant serine/threonine kinase by calcium and calcium/calmodulin. J. Biol. Chem. 271:8126-8132.
Tamura, K., Peterson, D., Peterson, N., Stecher, G., Nei, M., and Kumar, S. 2011. MEGA5: Molecular evolutionary genetics analysis using maximum likelihood, evolutionary distance, and maximum parsimony methods. Mol. Biol. Evol. 28:2731-2739.
Tirichine, L., Imaizumi-Anraku, H., Yoshida, S., Murakami, Y., Madsen, L. H., Miwa, H., Nakagawa, T., Sandal, N., Albrektsen, A. S., Kawaguchi, M., Downie, A., Sato, S., Tabata, S., Kouchi, H., Parniske, M., Kawasaki, S.,

and Stougaard, J. 2006. Deregulation of a Ca^{2+}/calmodulin-dependent kinase leads to spontaneous nodule development. Nature 441:1153-1156.
Urbański, D. F., Małolepszy, A., Stougaard, J., and Andersen, S. U. 2012. Genome-wide LORE1 retrotransposon mutagenesis and high-throughput insertion detection in Lotus japonicus. Plant J. 69:731-741.
Velten, M., Villoutreix, B. O., and Ladjimi, M. M. 2000. Quaternary structure of the HSC70 cochaperone HIP. Biochemistry 39:307-315.
Verdier, J., Torres-Jerez, I., Wang, M., Andriankaja, A., Allen, S. N., He, J., Tang, Y., Murray, J. D., and Udvardi, M. K. 2013. Establishment of the *Lotus japonicus* Gene Expression Atlas (LjGEA) and its use to explore legume seed maturation. Plant J. 74:351-362.
Waadt, R., Schmidt, L. K., Lohse, M., Hashimoto, K., Bock, R., and Kudla, J. 2008. Multicolor bimolecular fluorescence complementation reveals simultaneous formation of alternative CBL/CIPK complexes in planta. Plant J. 56:505-516.
Webb, M. A., Cavaletto, J. M., Klanrit, P., and Thompson, G. A. 2001. Orthologs in *Arabidopsis thaliana* of the Hsp70 interacting protein Hip. Cell Stress Chaperones 6:247-255.
Yano, K., Yoshida, S., Müller, J., Singh, S., Banba, M., Vickers, K., Markmann, K., White, C., Schuller, B., Sato, S., Asamizu, E., Tabata, S., Murooka, Y., Perry, J., Wang, T. L., Kawaguchi, M., Imaizumi-Anraku, H., Hayashi, M., and Parniske, M. 2008. CYCLOPS, a mediator of symbiotic intracellular accommodation. Proc. Natl. Acad. Sci. U.S.A. 105:20540-20545.
Zhu, H., Chen, T., Zhu, M., Fang, Q., Kang, H., Hong, Z., and Zhang, Z. 2008. A novel ARID DNA-binding protein interacts with SymRK and is expressed during early nodule development in *Lotus japonicus*. Plant Physiol. 148:337-347.

AUTHOR-RECOMMENDED INTERNET RESOURCES

The Gene Index Project: compbio.dfci.harvard.edu/tgi
The *Lotus japonicus* Gene Expression Atlas (LjGEA) Project: ljgea.noble.org/v2